Eur Spine J (2010) 19:1771–1775
DOI 10.1007/s00586-010-1430-x

ORIGINAL ARTICLE

MR/CT image fusion of the spine after spondylodesis: a feasibility study

C. A. Karlo · I. Steurer-Dober · M. Leonardi · C. W. A. Pfirrmann · M. Zanetti · J. Hodler

Received: 30 January 2010 / Revised: 22 April 2010 / Accepted: 2 May 2010 / Published online: 15 May 2010

Abstract The objective of this study is to evaluate feasibility, accuracy and time requirements of MR/CT image fusion of the lumbar spine after spondylodesis. Sagittal MR and CT images derived from standard imaging protocols (sagittal T2-weighted MR/sagittal reformatted multi-planar-reformation of the CT) of the lumbar spine with correct ($n = 5$) and incorrect ($n = 5$) implant position were fused by two readers (R1, R2) using OsiriX in two sessions placing one (session 1) or two (session 2) reference point(s) on the dorsal tip(s) of the cranial and caudal endplates from the second lumbar to the first sacral vertebra. R1 was an experienced musculoskeletal radiologist; R2 a spine surgeon, both had received a short training on the software tool. Fusion times and fusion accuracy, defined as the largest deviation between MR and CT in the median sagittal plane on the ventral tip of the cranial end plate of the most cranial vertebra visible on the CT, were measured in both sessions. Correct or incorrect implant position was evaluated upon the fused images for all patients by an experienced senior staff musculoskeletal radiologist. Mean fusion time (session 1/session 2; in seconds) was 100.4/95 (R1) and 104.2/119.8 (R2). Mean fusion deviation (session 1/session 2; in mm) was 1.24/2.20 (R1) and 0.79/1.62 (R2). The correct/incorrect implant position was identified correctly in all cases. In conclusion, MR/CT image fusion of the spine with metallic implants is feasible, fast, accurate and easy to implement in daily routine work.

Keywords Image fusion · MRI · CT · Lumbar spine · Spondylodesis

C. A. Karlo · I. Steurer-Dober · C. W. A. Pfirrmann · M. Zanetti · J. Hodler
Department of Radiology, University Hospital Balgrist, Forchstrasse 340, 8008 Zurich, Switzerland

C. A. Karlo (✉)
Institute for Diagnostic Radiology, University Hospital Zurich, Raemistrasse 100, 8091 Zurich, Switzerland
e-mail: christoph.karlo@usz.ch

I. Steurer-Dober
Institute of Radiology, Kantonsspital Luzern, 6000 Luzern 16, Switzerland

M. Leonardi
Department of Orthopedic Surgery, University Hospital Balgrist, Forchstrasse 340, 8008 Zurich, Switzerland

Introduction

Fusion of magnetic resonance (MR)- and computed tomography (CT)-derived images has been implemented in cardiac imaging [1–5], spinal radiosurgery [6] and computer-assisted craniofacial surgery [7–9] over the last years. However, only limited data are available regarding musculoskeletal MR/CT image fusion [10, 11]. MR imaging of the postoperative spine suffers from susceptibility artifacts caused by metallic implants. Therefore, assessment of integrity and correct position of metal installations is almost impossible. On the other hand, MR imaging is the method of choice for the evaluation of soft tissue structures. CT is considered the diagnostic imaging modality of choice to evaluate metal implants for possible disruption or incorrect placement, whereas the quality of soft tissue information is considered to be below MR standards. To combine the soft tissue information of MR imaging with the information about implants and bone provided by CT is practically relevant.

The purpose of our study was to evaluate the feasibility, accuracy and additional time requirements of MR/CT image fusion of the lumbar spine after spondylodesis using a free, open source post-processing software tool.

Materials and methods

Institutional review board approval was granted based on a general waiver, taking into account that patients have the possibility to choose if their data can be used for retrospective investigations or not.

Patients

Between January 2008 and November 2008, 45 consecutive patients had both an MR and CT examination of the lumbar spine at our institution. Twenty-three of them were examined by both modalities on the same day, within the routine postoperative follow up procedure. Of these 23 patients, 19 had metallic implants in their lumbar spines after spondylodesis. Implant position was reported to be correct in 14 patients and incorrect in five patients. These five patients with incorrect implant position as well as five patients with correct implant position were included in our study. Two senior musculoskeletal radiologists (YY, blinded, 14 years of experience with cross-sectional imaging of the spine, and ZZ, blinded, 20 years of experience) confirmed the correct ($n = 5$) or incorrect ($n = 5$) metal position using all available clinical and radiological information before the patients were included in the study.

Imaging

Imaging protocols for both MR and CT corresponded to the standard operating procedures of our institution. The indications for both scans had been made by the surgeons responsible for following the patients. For all MR imaging, a 1.5 T Scanner (Avanto, Espree or Symphony, Siemens Medical Solutions, Erlangen, Germany) was used. All CT examinations were performed on a 40 detector row CT scanner (Brilliance CT 40, Philips Medical Systems, Eindhoven, The Netherlands). The MR protocol included sagittal T1- and T2-weighted as well as transverse T2-weighted sequences angled into the intervertebral spaces individually. A detailed description of MR scanning parameters of the used sequence is provided in Table 1. Multi-planar reformations (MPR) of the CT data were obtained with a reconstruction slice thickness of 2 mm and a reconstruction increment of 1 mm in transverse, sagittal and coronal planes, as described in Table 2.

Table 1 MR imaging parameter

Parameter	Sagittal T2-weighted fast spin echo
Repetition time (ms)	3,740
Echo time (ms)	118
Flip angle (deg)	150
Field of view (mm)	300
Matrix	512/256
Number of signals acquired	12
Section thickness (mm)	4
Gap (%)	10

Table 2 CT imaging parameters

Parameter	CT of the lumbar spine
Tube voltage (kV)	140
Tube current time product (mAs)	300
Collimation	40 × 0.625
Pitch	0.675
Matrix	512/512
Reconstruction slice thickness (mm)	2.0
Reconstruction increment (mm)	1.0

Image fusion

The sagittal T2-weighted MR sequence and the sagittal MPR of the CT were transferred from the PACS (picture archive and communications system) to a separate workstation (MacPro, Apple, Cupertino, CA, USA) featuring OsiriX, a free and open source post-processing and fusion software tool [12–15]. Two readers received a short training on the software before they started with the two image fusion sessions. Reader 1 (R1) was a fellowship-trained musculoskeletal radiologist (DD, blinded, 5 years of cross-sectional image interpretation experience). Reader 2 (R2) was a senior staff spine surgeon (LL, blinded, no formal training in cross-sectional image interpretation but with practical experience in outpatient clinics and surgical planning). Both readers were blinded to the results of each other and did not have access to clinical information of the ten patients that were arranged in a work list on OsiriX. Both readers performed two image fusion sessions: In session 1 (one-point registration), they positioned one registration point per vertebra on the dorsal corner of the cranial endplate from the second lumbar vertebra through to the first sacral vertebra in the midsagittal image of the sagittal T2-weighted MR sequence and the sagittal MPR of the CT. In session 2 (two-point registration), they placed two reference points per vertebra on the dorsal corners of the cranial and caudal endplates from the second lumbar

vertebra through to the first sacral vertebra. All reference points were automatically numbered by the software in the order they had been placed and the exact same order had to be chosen for both imaging modalities to enable image registration, which was necessary to adapt the dimensions of the CT dataset to the dimensions of the MR dataset regarding slice thickness and image size. The registration was accomplished by an algorithm which compared the position of the reference points and adjusted the sagittal CT dataset to the MR dataset. The last step was to fuse the CT series onto the MR series, using the same software [12–15]. After image fusion, separate adjustment of window level settings was possible for the MR and CT part of the fused images. In the resulting fused image series, the CT part was color scale coded and the MR part gray scale coded. The window/level settings of the CT were adjusted to highlight cortical bone, any calcifications and metallic implants. The MR window/level settings were adjusted to optimize soft tissue contrast with regard to intervertebral foramina and nerve roots as well as intervertebral discs. Fusion times and accuracy were measured for both readers in both sessions by one of the authors not involved in the image fusion processes (AA, blinded). Fusion time was measured from opening OsiriX until archiving the fused images into the PACS after the fusion sessions. Fusion accuracy was defined as the greatest deviation between MR and CT images in the midsagittal plane at the ventral corner of the cranial endplate of the most cranial vertebra included in the CT examination in order to create a standardized measurement. After all fusion imaging sessions, a senior musculoskeletal radiologist (XX, blinded, 18 years of experience) evaluated the fused images of both image fusion sessions for correct or incorrect metal position and the results were compared to the inclusion criteria defined by the initial assessment of the two senior musculoskeletal radiologists (YY, ZZ), which served as the standard of reference for this match/mismatch analysis. Imaging examples are demonstrated in Figs. 1, 2, 3.

Results

The mean fusion time for the one-point registration was 100 s (range 76–180 s) for reader 1 and 104 s (range 63–145 s) for reader 2, whereas the mean fusion time for the two-point registration was 95 s (range 58–180 s) for reader 1 and 119 s (range 88–176 s) for reader 2, respectively.

The mean deviation of fusion accuracy of the one-point registration was 1.24 mm (range 0–2.77 mm) for reader 1 and 0.79 mm (range 0–1.20 mm) for reader 2, whereas the mean deviation of fusion accuracy of the two-point registration was 2.20 mm (range 0–4.50 mm) for reader 1 and 1.62 mm (range 0.7–2.6 mm) for reader 2.

The correct ($n = 5$) and incorrect ($n = 5$) metal placement was identified correctly in a final image analysis session by a senior musculoskeletal radiologist (XX) in all ten cases.

Discussion

Image fusion became popular in diagnostic imaging with the introduction of positron emission tomography (PET)–CT fusion [16, 17], which is now considered a routine application in nuclear medicine. Similarly, in cardiac radiology, image fusion is becoming more important by combining CT information about coronary artery disease and MR information about myocardial perfusion [3, 18, 19]. The fusion of CT and MR data sets has also been employed in radiation therapy for a better delineation of

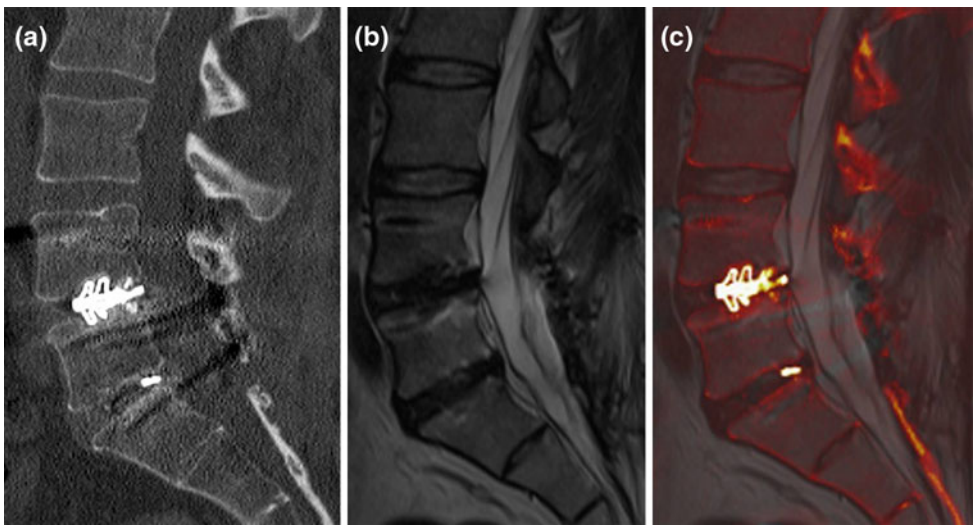

Fig. 1 An image fusion example between sagittal reformatted CT and sagittal T2-weighted MR images. The intervertebral cage L4/5 and a small piece of metal are well depicted on the CT (**a**) and fused image (**c**), whereas MR rules out disc degeneration of the L5/S1 segment (**b**). Information from both modalities are combined on the fused image (**c**)

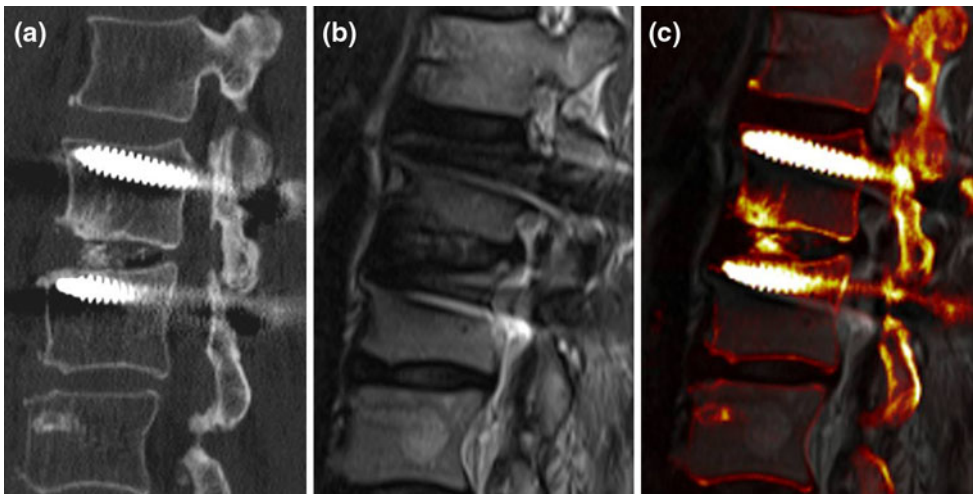

Fig. 2 An image fusion example between sagittal reformatted CT and sagittal T2-weighted MR images. The two screws in L2 and L3 are positioned close to the cranial endplates, which are intact. The calcifications in the intervertebral disc L2/3 are clearly depicted by the CT (**a**) and the fused images (**c**), whereas the intervertebral foramen including the nerve root is shown by the MR (**b**) and fused images (**c**). Information from both modalities is combined on one image (**c**)

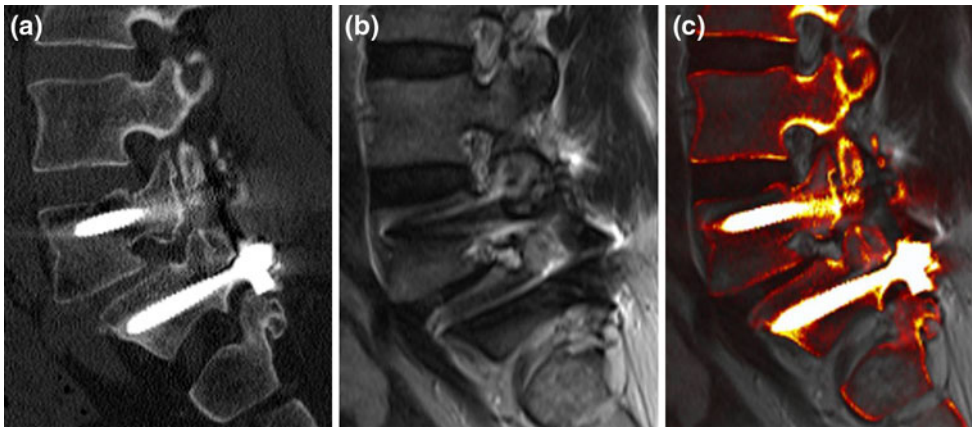

Fig. 3 An image fusion example between sagittal reformatted CT and sagittal T2-weighted MR images. The two screws in L5 and S1 are correctly placed, which is demonstrated by the CT (**a**) and fused images (**c**). Although anterolisthesis is present between L5 and S1, the intervertebral nerve root is neither compressed nor irritated by metal or osseous structures, as shown by the MR (**b**) and fused images (**c**). Important information from both modalities is combined on one image (**c**)

the desired target field [20] and in craniofacial surgery in order to improve computer-assisted guidance during surgery [6–9, 21]. In musculoskeletal radiology, however, image fusion has rarely been described [10]. The assessment of metal structures such as spondylodesis material is nearly impossible in MR due to severe susceptibility artifacts. However, MR provides important soft tissue information about possible intervertebral disc pathologies, compression of spinal nerve roots, the condition of the spinal cord, the presence of postoperative disorders such as hematoma or the presence of adjacent degeneration to the metal implants such as disc degeneration caused by a misplaced screw. CT is considered the imaging modality of choice when evaluating metal implants for their integrity and correct placement. In addition, CT is capable of quantifying intervertebral ossification processes and rule out possible adjacent fractures. However, CT provides less soft tissue information than MR.

In our study, we have evaluated an approach of combining the diagnostic power of MR and CT in one image series. We have demonstrated that fusion of CT and MR derived images of the spine with metallic implants is feasible, accurate and easy to learn. Based on our preliminary data set consisting of ten patients, the fusion times of the one- and two-point registrations were comparable. All image fusion sessions were performed by a radiologist and a spine surgeon in our study. Since handling the software is easy to learn, image fusion sessions might also be performed by technical staff, which would take away the time effort from the radiologist completely. Then fused images, given the fact that both examinations, CT and MR, were performed on the same day, can be a valuable add-on for the radiologist but also for the clinician to check for the postoperative situation. Regarding fusion accuracy, the one-point registration showed superior results when compared to the two-point registration due to a dedicated

algorithm of the fusion software that works better with fewer registration points [12–15, 22]. Although diagnostic information of CT and MR were combined on one image, we assume that fused images are not superior to MR and CT alone when considering diagnostic accuracy. However, the correct or incorrect position of metal implants of the lumbar spine can reliably be assessed on fused images, as we have shown. As CT is considered the standard of reference in the evaluation of the position of metal implants of the spine, MR imaging is superior in the evaluation of soft tissue abnormalities such as degenerative disc disease. However, the combination of both modalities on one image could yield the ability to diagnose multiple findings such as misplaced screws (CT information) and disc degeneration adjacent to fused segments (MR information) faster and more convincing. We were limited to a small study population of just ten patients. Therefore, further studies with larger populations should be performed to evaluate the diagnostic power of fused images of the spine after spondylodesis.

Conclusion

We conclude from our study that MR/CT image fusion of the spine with metallic implants after spondylodesis is feasible, fast, accurate and easy to implement in daily routine work.

References

1. Dickfeld T, Lei P, Dilsizian V, Jeudy J, Dong J, Voudouris A, Peters R, Saba M, Shekhar R, Shorofsky S (2008) Integration of three-dimensional scar maps for ventricular tachycardia ablation with positron emission tomography-computed tomography. JACC Cardiovasc Imaging 1:73–82. doi:10.1016/j.jcmg.2007.10.001
2. Gaemperli O, Schepis T, Valenta I, Husmann L, Scheffel H, Duerst V, Eberli FR, Luscher TF, Alkadhi H, Kaufmann PA (2007) Cardiac image fusion from stand-alone SPECT and CT: clinical experience. J Nucl Med 48:696–703. doi:10.2967/jnumed.106.037606
3. Gaemperli O, Schepis T, Kalff V, Namdar M, Valenta I, Stefani L, Desbiolles L, Leschka S, Husmann L, Alkadhi H, Kaufmann PA (2007) Validation of a new cardiac image fusion software for three-dimensional integration of myocardial perfusion SPECT and stand-alone 64-slice CT angiography. Eur J Nucl Med Mol Imaging 34:1097–1106. doi:10.1007/s00259-006-0342-9
4. Di Carli MF, Dorbala S (2007) Cardiac PET-CT. J Thorac Imaging 22:101–106. doi:10.1097/RTI.0b013e3180317a83
5. Makela T, Pham QC, Clarysse P, Nenonen J, Lotjonen J, Sipila O, Hanninen H, Lauerma K, Knuuti J, Katila T, Magnin IE (2003) A 3-D model-based registration approach for the PET, MR and MCG cardiac data fusion. Med Image Anal 7:377–389
6. Sohn MJ, Lee DJ, Yoon SW, Lee HR, Hwang YJ (2009) The effective application of segmental image fusion in spinal radiosurgery for improved targeting of spinal tumours. Acta Neurochir (Wien) 151:231–238. doi:10.1007/s00701-009-0210-z (discussion 238)
7. Nakamura M, Stover T, Rodt T, Majdani O, Lorenz M, Lenarz T, Krauss JK (2009) Neuronavigational guidance in craniofacial approaches for large (para)nasal tumors involving the anterior skull base and upper clival lesions. Eur J Surg Oncol 35:666–672. doi:10.1016/j.ejso.2008.10.011
8. Wong KC, Kumta SM, Antonio GE, Tse LF (2008) Image fusion for computer-assisted bone tumor surgery. Clin Orthop Relat Res 466:2533–2541. doi:10.1007/s11999-008-0374-5
9. Nemec SF, Peloschek P, Schmook MT, Krestan CR, Hauff W, Matula C, Czerny C (2008) CT-MR image data fusion for computer-assisted navigated surgery of orbital tumors. Eur J Radiol. doi:10.1016/j.ejrad.2008.11.003
10. Kaminsky J, Rodt T, Zajaczek J, Donnerstag F, Zumkeller M (2004) Multisegmental image fusion of the spine. Biomed Tech (Berl) 49:49–55. doi:10.1515/BMT.2004.010
11. Chen YT, Wang MS (2004) Three-dimensional reconstruction and fusion for multi-modality spinal images. Comput Med Imaging Graph 28:21–31
12. Jalbert F, Paoli JR (2008) Osirix: free and open-source software for medical imagery. Rev Stomatol Chir Maxillofac 109:53–55. doi:10.1016/j.stomax.2007.07.007
13. Rosset A, Spadola L, Pysher L, Ratib O (2006) Informatics in radiology (infoRAD): navigating the fifth dimension: innovative interface for multidimensional multimodality image navigation. Radiographics 26:299–308. doi:10.1148/rg.261055066
14. Rosset A, Spadola L, Ratib O (2004) OsiriX: an open-source software for navigating in multidimensional DICOM images. J Digit Imaging 17:205–216. doi:10.1007/s10278-004-1014-6
15. Rosset C, Rosset A, Ratib O (2005) General consumer communication tools for improved image management and communication in medicine. J Digit Imaging 18:270–279. doi:10.1007/s10278-005-6703-2
16. Wahl RL, Quint LE, Greenough RL, Meyer CR, White RI, Orringer MB (1994) Staging of mediastinal non-small cell lung cancer with FDG PET, CT, and fusion images: preliminary prospective evaluation. Radiology 191:371–377
17. Wahl RL, Quint LE, Cieslak RD, Aisen AM, Koeppe RA, Meyer CR (1993) "Anatometabolic" tumor imaging: fusion of FDG PET with CT or MRI to localize foci of increased activity. J Nucl Med 34:1190–1197
18. Young AA, French BA, Yang Z, Cowan BR, Gilson WD, Berr SS, Kramer CM, Epstein FH (2006) Reperfused myocardial infarction in mice: 3D mapping of late gadolinium enhancement and strain. J Cardiovasc Magn Reson 8:685–692. doi:10.1080/10976640600721767
19. Setser RM, O'Donnell TP, Smedira NG, Sabik JF, Halliburton SS, Stillman AE, White RD (2005) Coregistered MR imaging myocardial viability maps and multi-detector row CT coronary angiography displays for surgical revascularization planning: initial experience. Radiology 237:465–473. doi:10.1148/radiol.2372040236
20. Dalah EZ, Nisbet A, Reise S, Bradley D (2008) Evaluating commercial image registration packages for radiotherapy treatment planning. Appl Radiat Isot 66:1948–1953. doi:10.1016/j.apradiso.2008.06.003
21. Nemec SF, Donat MA, Mehrain S, Friedrich K, Krestan C, Matula C, Imhof H, Czerny C (2007) CT-MR image data fusion for computer assisted navigated neurosurgery of temporal bone tumors. Eur J Radiol 62:192–198. doi:10.1016/j.ejrad.2006.11.029
22. Nishie A, Stolpen AH, Obuchi M, Kuehn DM, Dagit A, Andresen K (2008) Evaluation of locally recurrent pelvic malignancy: performance of T2- and diffusion-weighted MRI with image fusion. J Magn Reson Imaging 28:705–713. doi:10.1002/jmri.21486